

A New Optimal Scheme for Solving Nonlinear Heat Conduction Problems

Chih-Wen Chang^{1,2}, Chein-Shan Liu³

Abstract: In this article, we utilize an optimal vector driven algorithm (OVDA) to cope with the nonlinear heat conduction problems (HCPs). From this set of nonlinear ordinary differential equations, we propose a purely iterative scheme and the spatial-discretization of finite difference method for revealing the solution vector \mathbf{x} , without having to invert the Jacobian matrix \mathbf{D} . Furthermore, we introduce three new ideas of bifurcation, attracting set and optimal combination, which are restrained by two parameters γ and α . Several numerical instances of nonlinear systems under noise are examined, finding that the OVDA has a fast convergence rate, great computation accuracy and efficiency.

Keywords: Nonlinear algebraic equations, Nonlinear heat conduction equation, Iterative algorithm, Optimal vector driven algorithm (OVDA), Invariant manifold

1 Introduction

Heat conduction problems that appear from engineering applications are often categorized as linear heat conduction problems and nonlinear heat conduction problems (HCPs). In most situations, solving those problems analytically and exactly is impossible, or at least highly impractical. Hence, numerical algorithms such as finite difference method (FDM) and finite element method (FEM) are often employed to estimate the linear HCPs [Necati Özisik (1994); Zienkiewicz, Taylor and Zhu (2005)]. Because the mesh establishment of domain is time-consuming and cannot always be totally automated, [Zhu, Liu and Lu (1998); Bulgakov, Sarler and Kuhn (1998); Zhu (1998); Sutradhar, Paulino and Gray (2002); Bialecki, Jurgas and Kuhn (2002); Zerroukat (1999)] employed the boundary element method (BEM) to solve the linear HCPs. However, the mesh generation of boundary increases the computation time and capacity necessity. Comparing with those mesh-dependent schemes

¹ Computing Technology Integration Division, National Center for High-Performance Computing, Taichung 40763, Taiwan

² Corresponding author, Tel.:+886-4-24620202#860. *E-mail address:* 0903040@nchc.narl.org.tw

³ Department of Civil Engineering, National Taiwan University, Taipei 10617, Taiwan

like as FDM, FEM and BEM, the meshless approaches [Chantasiriwan (2006); Walker (1992); Johansson and Lesnic (2008)], which do not need any domain or boundary discretization, have been proposed.

For the nonlinear HCPs, Zokayi, Hadizadeh, Darania and Rajabi (2006) analyzed the RF-pair method for the relation between the Emden-Fowler equation and the nonlinear heat conduction problem with the variable transfer coefficient. This scheme demonstrates that, under the RF-pair operations, the solution of transformed equation can be changed into the solution of the mention equation. Nevertheless, they did not show the numerical results and mention how the initial data were disturbed by noise. Recently, Chu and Chen (2008) have used the hybrid method of differential transform and finite difference scheme to solve the transient responses of a nonlinear heat conduction problem; however, this study did not discuss how the initial data were perturbed by noise.

This research is organized as follows. Section 2 demonstrates a theoretical basis of the proposed scheme. We begin from a continuous manifold defined in terms of residual-norm, and arrive at a system of ordinary differential equations (ODEs) driven by a vector, which is a combination of the vectors \mathbf{E} and $\mathbf{D}^T\mathbf{E}$, where \mathbf{D} is the Jacobian. Section 3 is dedicated to deriving a scalar equation to keep the discretely iterative orbit on the manifold, and then we propose two new concepts of bifurcation and optimization to choose the weighting factor and optimal parameter α , which automatically have a convergent behavior of the residual-error curve. In Section 4, we employ the present approach with different weighting factors and combination parameters to resolve three numerical experiments. At last, some concluding remarks are drawn in Section 5.

2 An invariant manifold

In this study, we propose a new iterative approach to solve a system of nonlinear algebraic equations (NAEs): $E_i(x_1, \dots, x_n) = 0, i = 1, \dots, n$, or in their vector-form:

$$\mathbf{E}(\mathbf{x}) = \mathbf{0}. \quad (1)$$

For the NAEs in Eq. (1), we can formulate a scalar Newton homotopy function:

$$g(\mathbf{x}, t) = \frac{Q(t) \|\mathbf{E}(\mathbf{x})\|^2}{2} - \frac{\|\mathbf{E}(\mathbf{x}_0)\|^2}{2} = 0, \quad (2)$$

in which, let \mathbf{x} be a function of a fictitious time-like variable t , and its initial value is $\mathbf{x}(0) = \mathbf{x}_0$.

We anticipate $g(\mathbf{x}, t) = 0$ to be an invariant manifold in the space of (\mathbf{x}, t) for a dynamical system $g(\mathbf{x}(t), t) = 0$ to be specified further. While $Q > 0$, the

manifold clarified by Eq. (2) is continuous, and therefore the following operation of differential accomplished on the manifold makes sense [Liu and Atluri (2011a)]. As a “consistency condition”, by taking the time differential of Eq. (2) with respect to t and contemplating $\mathbf{x} = \mathbf{x}(t)$, we obtain

$$\frac{\dot{Q}(t) \|\mathbf{E}(\mathbf{x})\|^2}{2} - Q(t)(\mathbf{D}^T \mathbf{E}) \cdot \dot{\mathbf{x}} = 0. \tag{3}$$

We presume that the evolution of \mathbf{x} is driven by a vector \mathbf{w} :

$$\dot{\mathbf{x}} = \lambda \mathbf{w}, \tag{4}$$

where λ in general is a scalar function of t , and

$$\mathbf{w} = \alpha \mathbf{E} + (1 - \alpha) \mathbf{D}^T \mathbf{E}, \tag{5}$$

is a suitable combination of the residual vector \mathbf{E} as well as gradient vector $\mathbf{D}^T \mathbf{E}$, and is α a parameter to be optimized below. Inserting Eq. (4) into Eq. (3), we can derive

$$\dot{\mathbf{x}} = -p(t) \frac{\|\mathbf{E}\|^2}{\mathbf{E}^T \mathbf{q}} \mathbf{w}, \tag{6}$$

in which

$$\mathbf{F} := \mathbf{D} \mathbf{D}^T, \tag{7}$$

$$\mathbf{q} := \mathbf{D} \mathbf{w} = \mathbf{q}_1 + \alpha \mathbf{q}_2 = \mathbf{F} \mathbf{E} + \alpha (\mathbf{D} - \mathbf{F}) \mathbf{E}, \tag{8}$$

$$p(t) := \frac{\dot{Q}(t)}{2Q(t)}. \tag{9}$$

Thus, in this algorithm if $Q(t)$ can be guaranteed to be a monotonically increasing function of t , we may have an absolutely convergent property in solving the NAEs in Eq. (1):

$$\|\mathbf{E}(\mathbf{x})\|^2 = \frac{C}{Q(t)}, \tag{10}$$

where

$$C = \|\mathbf{E}(\mathbf{x}_0)\|^2 \tag{11}$$

is chosen by the initial value \mathbf{x}_0 . We do not require to specify the function $Q(t)$ a priori; however, $\sqrt{C/Q(t)}$ only acts as a measure of the residual error of \mathbf{E} at the same time. Therefore, we impose on our scheme that $Q(t) > 0$ is a monotonically increasing function of t . When t is enormous, the above equation will compel the residual error $\|\mathbf{E}(\mathbf{x})\|$ to tend to zero, and meanwhile the solution of Eq. (1) is acquired accessibly.

3 Dynamics of the proposed iterative schemes

3.1 Discretizing, yet keeping x on the manifold

Now, we discretize the foregoing continuous time dynamics embodied in Eq. (6) into a discrete time dynamics:

$$\mathbf{x}(t + \Delta t) = \mathbf{x}(t) - \beta \frac{\|\mathbf{E}\|^2}{\mathbf{E}^T \mathbf{q}} \mathbf{w}, \tag{12}$$

where

$$\beta = p(t)\Delta t \tag{13}$$

is the step-length. Eq. (12) is acquired from the ODEs in Eq. (6) by employing the Euler algorithm.

To keep \mathbf{x} on the manifold defined by Eq. (10), we can contemplate the evolution of \mathbf{E} along the path $\mathbf{x}(t)$ by

$$\dot{\mathbf{E}} = \mathbf{D}\dot{\mathbf{x}} = -p(t) \frac{\|\mathbf{E}\|^2}{\mathbf{E}^T \mathbf{q}} \mathbf{q}. \tag{14}$$

Similarly, we utilize the Euler algorithm to integrate Eq. (14) and acquire

$$\mathbf{E}(t + \Delta t) = \mathbf{E}(t) - \beta \frac{\|\mathbf{E}\|^2}{\mathbf{E}^T \mathbf{q}} \mathbf{q}, \tag{15}$$

Taking the square-norms of both the sides of Eq. (15) and employing Eq. (10), we can acquire

$$\frac{C}{Q(t + \Delta t)} = \frac{C}{Q(t)} - 2\beta \frac{C}{Q(t)} + \beta^2 \frac{C}{Q(t)} \frac{\|\mathbf{E}\|^2}{(\mathbf{E}^T \mathbf{q})^2} \|\mathbf{q}\|^2. \tag{16}$$

Hence, we can derive the following scalar equation:

$$a_0 \beta^2 - 2\beta + 1 - \frac{Q(t)}{Q(t + \Delta t)} = 0, \tag{17}$$

where

$$a_0 := \frac{\|\mathbf{E}\|^2 \|\mathbf{q}\|^2}{(\mathbf{E}^T \mathbf{q})^2}. \tag{18}$$

Consequently, $g(\mathbf{x}, t) = 0, t \in \{0, 1, 2, \dots\}$ remains to be an invariant manifold in the space of (\mathbf{x}, t) for the discrete time dynamical system $g(\mathbf{x}(t), t) = 0$, which will be explored further in the next two sections. Liu and Atluri (2011a) first derived the formula (18) for a simply gradient-vector driven dynamical system.

3.2 A trial discrete dynamics

Presently, we specify the discrete time dynamics $g(\mathbf{x}(t), t) = 0, t \in \{0, 1, 2, \dots\}$, through specifying the discrete time dynamics of $Q(t), t \in \{0, 1, 2, \dots\}$. Note that discrete time dynamics is an iterative dynamics, which in turn amounts to an iterative approach.

We first utilize the Euler algorithm:

$$Q(t + \Delta t) = Q(t) + \dot{Q}(t)\Delta t. \tag{19}$$

Then from Eq. (9) we obtain

$$\beta = p(t)\Delta t = 0.5[G(t) - 1], \tag{20}$$

where the ratio $G(t)$ is defined by

$$G(t) = \frac{Q(t)}{Q(t + \Delta t)}. \tag{21}$$

As a necessity of $\dot{Q}(t) > 0$, we require $R(t) > 1$.

Therefore, through some operations, Eq. (17) becomes

$$a_0G^3(t) - (2a_0 + 4)G^2(t) + (a_0 + 8)G(t) - 4 = 0, \tag{22}$$

which can be further written as

$$[G(t) - 1]^2[a_0G(t) - 4] = 0. \tag{23}$$

Because $G = 1$ is a double root and does not satisfy $G > 1$, which is not the wanted one, we take

$$G(t) = \frac{4}{a_0} = \frac{4(\mathbf{E}^T \mathbf{q})^2}{\|\mathbf{E}\|^2 \|\mathbf{q}\|^2}. \tag{24}$$

By utilizing Eq. (20), Eq. (12) can be written as

$$\mathbf{x}(t + \Delta t) = \mathbf{x}(t) - 0.5[G(t) - 1] \frac{\|\mathbf{E}\|^2}{\mathbf{E}^T \mathbf{q}} \mathbf{w}. \tag{25}$$

However, this scheme has an unfortunate drawback in that when the iterated a_0 begins to close to 4 before it grows up a large value, the approach stagnates at a point which is not a necessary answer. We will evade following this kind of dynamics by developing a better dynamics as below. This denotes that the present method will confront this fate to lose its dynamics force if we stress the iterative orbit as being situated on the manifold clarified by Eq. (10). This idea has been first found by Liu and Atluri (2011a) for a gradient-driven approach.

3.3 A good discrete dynamics

Let

$$s = \frac{Q(t)}{Q(t + \Delta t)} = \frac{\|\mathbf{E}(\mathbf{x}(t + \Delta t))\|^2}{\|\mathbf{E}(\mathbf{x}(t))\|^2}, \tag{26}$$

which is a significant quantity to evaluate the convergence property of numerical scheme for solving NAEs. If s can be promised to be $s < 1$, then the residual error $\|\mathbf{E}\|$ will be decreased step-by-step.

From Eqs. (17) and (26), we can acquire

$$a_0\beta^2 - 2\beta + 1 - s = 0, \tag{27}$$

in which

$$a_0 := \frac{\|\mathbf{E}\|^2 \|\mathbf{q}\|^2}{(\mathbf{E}^T \mathbf{q})^2} \geq 1, \tag{28}$$

by employing the Cauchy-Schwarz inequality:

$$\mathbf{E}^T \mathbf{q} \leq \|\mathbf{E}\| \|\mathbf{q}\| .$$

From Eq. (27), we can obtain the solution of β to be

$$\beta = \frac{1 - \sqrt{1 - (1 - s)a_0}}{a_0}, \text{ if } 1 - (1 - s)a_0 \geq 0. \tag{29}$$

Let

$$1 - (1 - s)a_0 = \gamma^2 \geq 0, \tag{30}$$

$$s = 1 - \frac{1 - \gamma^2}{a_0}. \tag{31}$$

Hence, from Eq. (29) it follows that

$$\beta = \frac{1 - \gamma}{a_0}, \tag{32}$$

and from Eqs. (12) and (18) we can acquire the approach as follows:

$$\mathbf{x}(t + \Delta t) = \mathbf{x}(t) - \eta \frac{\mathbf{E}^T \mathbf{q}}{\|\mathbf{q}\|^2} \mathbf{w}, \tag{33}$$

in which

$$\eta = 1 - \gamma. \tag{34}$$

Here $0 \leq \gamma < 1$ is a weighting parameter. Then, in the numerical instances, we will interpret that γ plays a major role for the bifurcation of discrete dynamics. Under the above condition, we can prove that the new scheme satisfies

$$\frac{\|\mathbf{E}(t + \Delta t)\|}{\|\mathbf{E}(t)\|} = \sqrt{s} < 1, \tag{35}$$

which indicates that the residual error is absolutely decreased.

We do not need Δt to be integrated in the above method. Moreover, the property in Eq. (35) is pivotal because it promises the new scheme to be absolutely convergent to the true solution.

3.4 Optimal value for α

The scheme (33) does not specify how to determine the parameter α . One way is that α is determined by the user. Furthermore, we can choose a suitable α such that s clarified in Eq. (31) is minimized with respect to α , because a smaller s will result in a faster convergence as displayed in Eq. (35). The concept of optimizing α , was first developed by Liu and Atluri (2011b) for other scheme.

Therefore, by inserting Eq. (28) for a_0 into Eq. (31), we can obtain s as follows:

$$s = 1 - \frac{(1 - \gamma^2)(\mathbf{E} \cdot \mathbf{q})^2}{\|\mathbf{E}\|^2 \|\mathbf{q}\|^2}, \tag{36}$$

where q as defined by Eq. (8) includes a parameter α . Let $\partial s / \partial \alpha = 0$, and through some algebraic operations we can resolve α by

$$\alpha = \frac{(\mathbf{q}_1 \cdot \mathbf{E})(\mathbf{q}_1 \cdot \mathbf{q}_2) - (\mathbf{q}_2 \cdot \mathbf{E}) \|\mathbf{q}_1\|^2}{(\mathbf{q}_2 \cdot \mathbf{E})(\mathbf{q}_1 \cdot \mathbf{q}_2) - (\mathbf{q}_1 \cdot \mathbf{E}) \|\mathbf{q}_2\|^2}. \tag{37}$$

Remark 1: For the usual three-dimensional vectors $\mathbf{a}, \mathbf{b}, \mathbf{c} \in R^3$, the following formula is famous:

$$\mathbf{a} \times (\mathbf{b} \times \mathbf{c}) = (\mathbf{a} \cdot \mathbf{c})\mathbf{b} - (\mathbf{a} \cdot \mathbf{b})\mathbf{c}. \tag{38}$$

Liu (2000) has utilized a Jordan algebra by extending the above formula to vectors in n -dimension:

$$[\mathbf{a}, \mathbf{b}, \mathbf{c}] = (\mathbf{a} \cdot \mathbf{b})\mathbf{c} - (\mathbf{c} \cdot \mathbf{b})\mathbf{a}, \mathbf{a}, \mathbf{b}, \mathbf{c} \in R^n. \tag{39}$$

Hence α in Eq. (37) can be expressed as

$$\alpha = \frac{[\mathbf{q}_1, \mathbf{q}_2, \mathbf{E}] \cdot \mathbf{q}_1}{[\mathbf{q}_2, \mathbf{q}_1, \mathbf{E}] \cdot \mathbf{q}_2}. \tag{40}$$

The above parameter α can be called the optimal α because it brings us a new strategy to determine the best orientation to find the solution of NAEs. Furthermore, we have an explicit form to implement it into the numerical program, and therefore it is time-saving for calculating it.

3.5 Optimal value for α

Since the fictitious time variable is now discrete, $t \in \{0, 1, 2, \dots\}$, we let \mathbf{x}_k denote the numerical value of \mathbf{x} at the k -th step. Hence, we arrive at a purely iterative method through Eqs. (33) and (34):

$$\mathbf{x}_{k+1} = \mathbf{x}_k - (1 - \gamma) \frac{\mathbf{E}_k^T \mathbf{q}_k}{\|\mathbf{q}_k\|^2} \mathbf{w}_k. \tag{41}$$

After that, we devise the following scheme:

- (1) Choose $0 \leq \gamma < 1$, and give an initial guess of \mathbf{x}_0 .
- (2) For $k=0, 1, 2, \dots$ we repeat the following calculations:

$$\mathbf{q}_1^k = \mathbf{F}_k \mathbf{E}_k, \tag{42}$$

$$\mathbf{q}_2^k = (\mathbf{D}_k - \mathbf{F}_k) \mathbf{E}_k, \tag{43}$$

$$\alpha_k = \frac{[\mathbf{q}_1^k, \mathbf{q}_2^k, \mathbf{E}_k] \cdot \mathbf{q}_1^k}{[\mathbf{q}_2^k, \mathbf{q}_1^k, \mathbf{E}_k] \cdot \mathbf{q}_2^k}, \tag{44}$$

$$\mathbf{w}_k = \alpha_k \mathbf{E}_k + (1 - \alpha_k) \mathbf{D}_k^T \mathbf{E}_k \tag{45}$$

$$\mathbf{q}_k = \mathbf{D}_k \mathbf{w}_k \tag{46}$$

$$\mathbf{x}_{k+1} = \mathbf{x}_k - (1 - \gamma) \frac{\mathbf{E}_k \cdot \mathbf{q}_k}{\|\mathbf{q}_k\|^2} \mathbf{w}_k. \tag{47}$$

If \mathbf{x}_{k+1} converges according to a given stopping criterion $\|\mathbf{E}_{k+1}\| < \varepsilon$, then stop; otherwise, go to step (2).

4 Nonlinear heat conduction problems and numerical examples

We deliberate the following equations about the nonlinear HCP:

$$c(x)\frac{\partial u}{\partial t} = k(x)u_{xx} + k'(x)u_x + u^m + f(x, t), 0 \leq x \leq \ell, 0 \leq t \leq T, \quad (48)$$

with the boundary conditions

$$u(0, t) = g(t), u(\ell, t) = h(t), \quad (49)$$

and the initial condition

$$u(x, 0) = p(x). \quad (50)$$

where u is the temperature field of a rod, $k(x)$ is a thermal conductivity, ℓ is the length of a rod, and $f(x, t)$ is a linear function of x and t .

We will utilize the OVDA and the spatial-discretization of finite difference approach to the calculations of nonlinear HCP through numerical experiments. We are concerned about the stability of our scheme when the input initial measured data are polluted by random noise for different issues. We can evaluate the stability by increasing the different levels of random noise in the initial data:

$$\hat{u}_i = u_i + s[2R(i) - 1], \quad (51)$$

where u_i is the initial exact data. We use the function RANDOM_NUMBER given in Fortran to generate the noisy data $R(i)$, which are random numbers in $[-1, 1]$, and s means the level of absolute noise. Then, the final noisy data \hat{u}_i are employed in the calculations.

4.1 Example 1

In this example, we apply the proposed method involving the vector \mathbf{w} of Eq. (5) to solve the following one-dimensional nonlinear HCP:

$$u_t = x^3 u_{xx} + u^2 - 6x^4 e^t - x^6 e^{2t} + x^3 e^t, 0 \leq x \leq 1, 0 \leq t \leq T, \quad (52)$$

with the boundary conditions

$$u(0, t) = 0, u(1, t) = e^t, \quad (53)$$

and the initial condition

$$u(x, 0) = x^3. \quad (54)$$

The exact solution is

$$u(x,t) = x^3 e^t. \quad (55)$$

By applying the new algorithm to solve the above equation in the domain of $0 \leq x \leq 1$ and $0 \leq t \leq 1$, we use $n_1 = 17$ and $n_2 = 21$, which are numbers of nodal points in a standard finite difference approximation of Eq. (52). Because a_0 defined in Eq. (18) is a very important factor of our new algorithms, we show it in Fig. 1(b) for the present algorithm with $\gamma = 0$, while the residual error is shown in Fig. 1(a), and α is shown in Fig. 1(c) by the dashed lines. Under a convergence criterion $\varepsilon = 0.1$, the present algorithm with $\gamma = 0$ can also converge with 110 steps, and attains an accurate solution with the maximum error 6.33×10^{-3} . The optimal α varies in a narrow band with the range from 0.9981 to 0.9990, and a_0 approaches to a constant, which reveals an attracting set for the iterative orbit. Under the same convergence criterion, the present algorithm with $\gamma = 0.15$ converges much fast with only 104 steps. The residual error, a_0 and α are shown in Fig. 1 by the solid lines. By employing $\gamma = 0.15$ the value of a_0 does not tend to a constant, and its value is smaller than the a_0 obtained from the present algorithm with $\gamma = 0$ and optimal α , which is the main reason to cause the fast convergence of the present algorithm with $\gamma = 0.15$.

In this example, when the input initial measured data are disturbed by random noise, we are interested in the stability of OVDA, which is investigated by adding the level of random noise on the initial data. The results of $T = 1$ are compared with the numerical result without contemplating the absolute random noise in Fig. 2. Note that the absolute noise level with $s = 0.2$ perturbs the numerical solutions a little from that without adding the noise. The exact solutions and numerical solutions are plotted in Figs. 3(a)-(c) sequentially. Even under the large noise, the numerical solution indicated in Fig. 3(c) is a good approximation to the exact initial data as illustrated in Fig. 3(a).

4.2 Example 2

Then, we ponder the following one-dimensional nonlinear HCP:

$$u_t = (x-5)^3 u_{xx} + 3(x-5)^2 u_x + u^3 - 15(x-5)^4 e^{-t} - (x-5)^9 e^{-3t} - (x-5)^3 e^{-t}, \quad 0 \leq x \leq 1, 0 \leq t \leq T, \quad (56)$$

with the boundary conditions

$$u(0,t) = -125e^{-t}, \quad u(1,t) = -64e^{-t}, \quad (57)$$

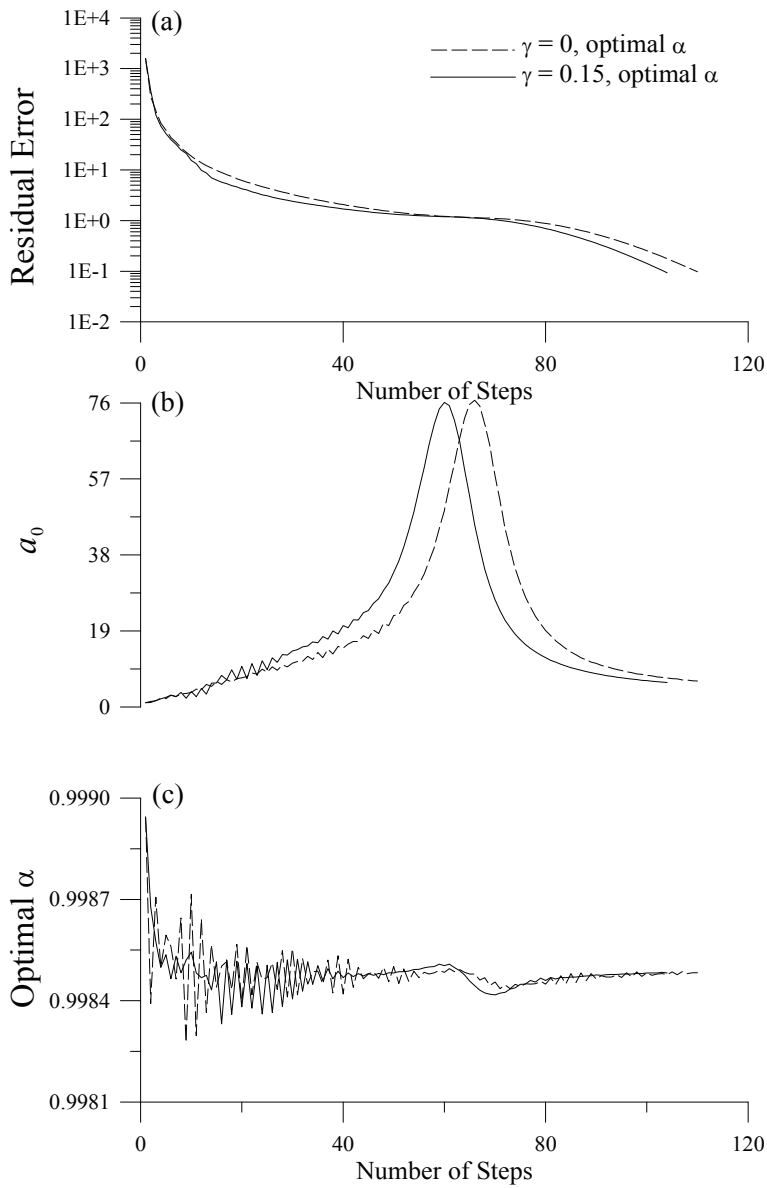


Figure 1: For example 1, with different α and γ , comparing residual errors, a_0 and α .

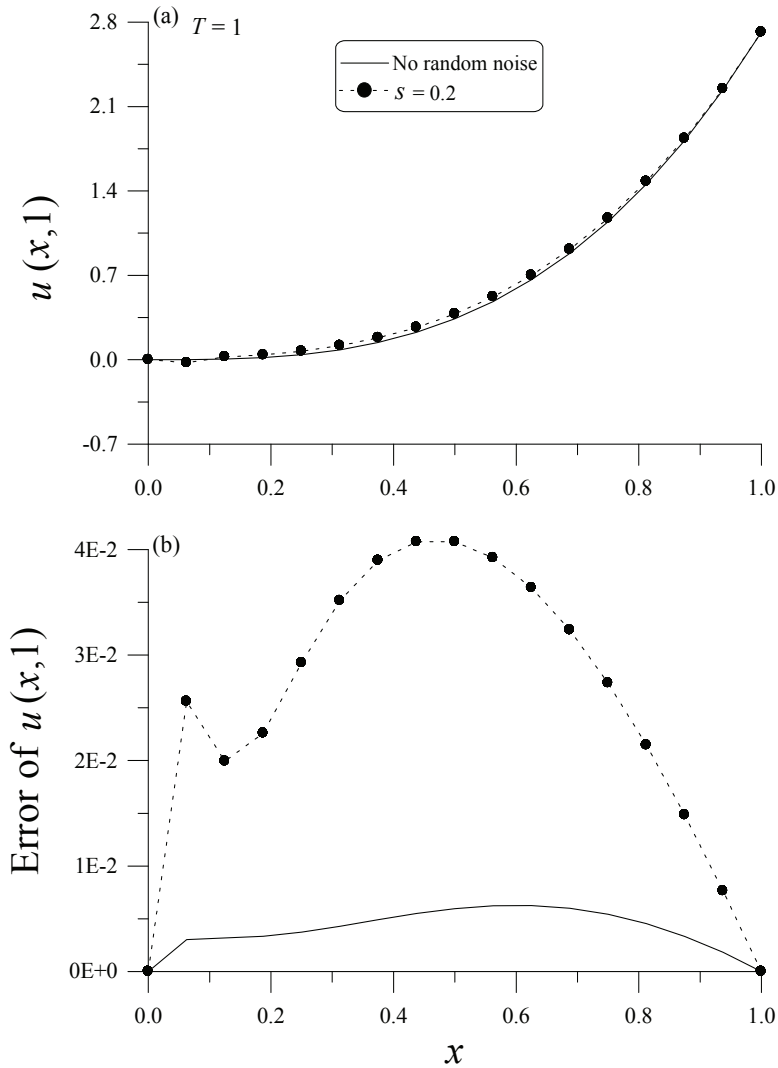


Figure 2: Comparisons of numerical solutions were made in (a) with different levels of noise $s = 0, 0.2$, and (b) the corresponding numerical errors.

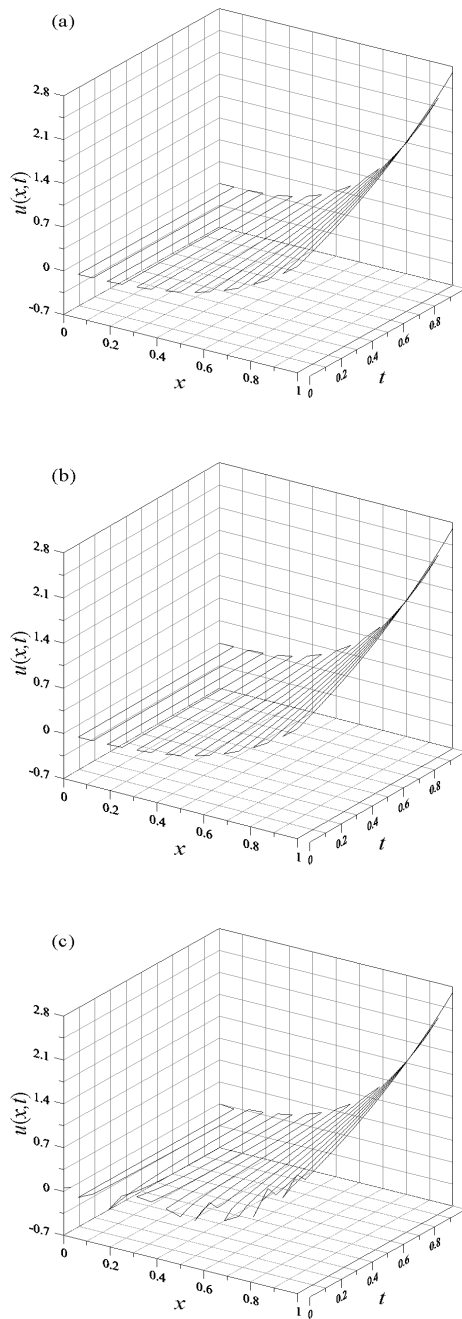


Figure 3: The exact solution for Example 1 of one-dimensional nonlinear HCP with $T = 1$ are shown in (a), in (b) the OVDA solution without random noise effect, and in (c) the OVDA solution with random noise.

and the initial condition

$$u(x, 0) = (x - 5)^3. \quad (58)$$

The exact solution is

$$u(x, t) = (x - 5)^3 e^{-t}. \quad (59)$$

By using the proposed scheme to tackle the above problem in the domain of $0 \leq x \leq 1$ and $0 \leq t \leq 10$, we employ $n_1 = 11$ and $n_2 = 19$, which are numbers of nodal points in a standard finite difference approximation of Eq. (56). Because a_0 defined in Eq. (18) is a very important factor of our new algorithms, we show it in Fig. 4(b) for the present algorithm with $\gamma = 0$, while the residual error is shown in Fig. 4(a), and α is shown in Fig. 4(c) by the dashed lines. Under a convergence criterion $\varepsilon = 0.01$, the present algorithm with $\gamma = 0$ can also converge with 103 steps, and attains an accurate solution with the maximum error 3.80×10^{-3} . The optimal α varies in a narrow band with the range from 0.99996 to 1.00004, and a_0 approaches to a constant, which reveals an attracting set for the iterative orbit. Under the same convergence criterion, the present algorithm with $\gamma = 0.14$ converges much fast with only 49 steps. The residual error, a_0 and α are shown in Fig. 4 by the solid lines. By employing $\gamma = 0.14$ the value of a_0 does not tend to a constant, and its value is smaller than the a_0 obtained from the present method with $\gamma = 0$ and optimal α , which is the main reason to cause the fast convergence of the proposed approach with $\gamma = 0.14$.

In this example, when the input initial measured data are perturbed by random noise, we are concerned about the stability of OVDA, which is investigated by adding the level of random noise on the initial data. The results of $T = 10$ are compared with the numerical result without contemplating the absolute random noise in Fig. 5. Note that the absolute noise level with $s = 1$ perturbs the numerical solutions a little from that without adding the noise, and the maximum error is 2.03×10^{-6} . The exact solutions and numerical solutions are plotted in Figs. 6(a)-(c) sequentially. Even under the large noise, the numerical solution indicated in Fig. 6(c) is a good approximation to the exact initial data as exhibited in Fig. 6(a).

4.3 Example 3

Let us further consider another one-dimensional highly nonlinear HCP:

$$x^6 u_t = (x - 3)^6 u_{xx} - 6(x - 3)^5 u_x - u^3 - x^3 u^2 + 6(x - 3)^{10} e^{-2t} + x^3 (x - 3)^{12} e^{-4t} + (x - 3)^{18} e^{-6t} - 2x^6 (x - 3)^6 e^{-2t}, \quad 0 \leq x \leq 1, 0 \leq t \leq T, \quad (60)$$

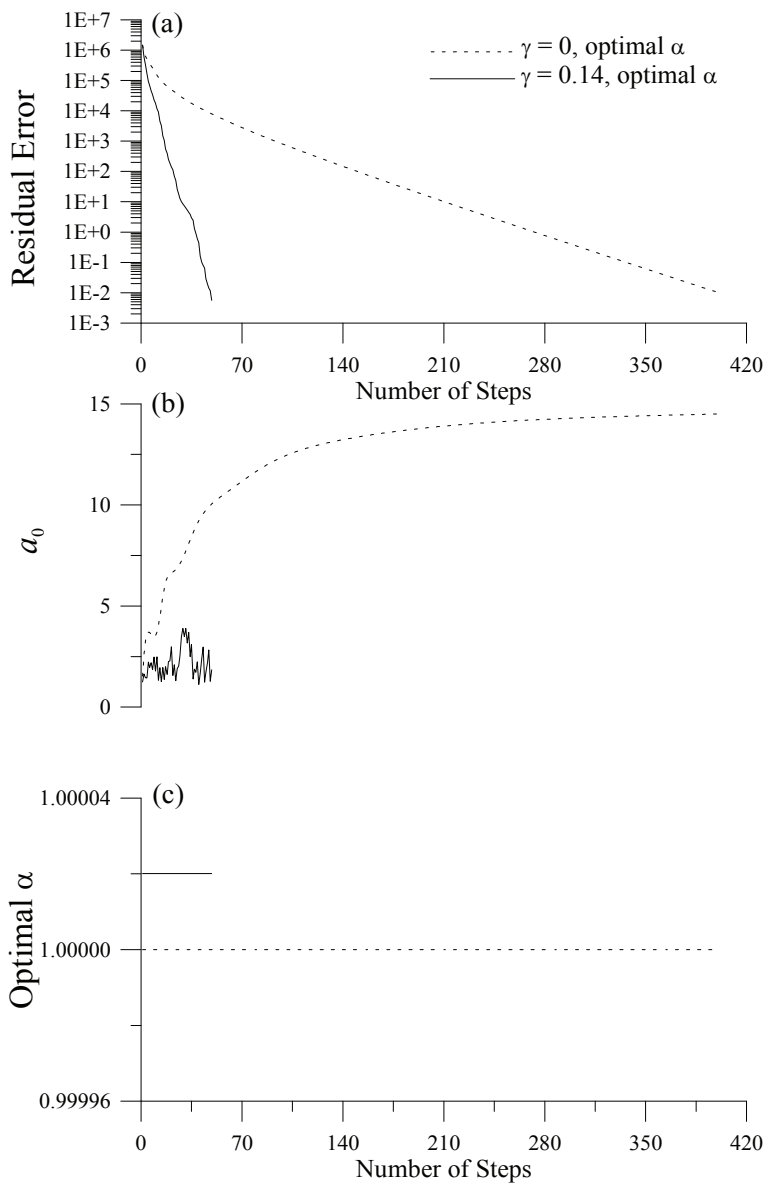


Figure 4: For example 2, with different α and γ , comparing residual errors, a_0 and α .

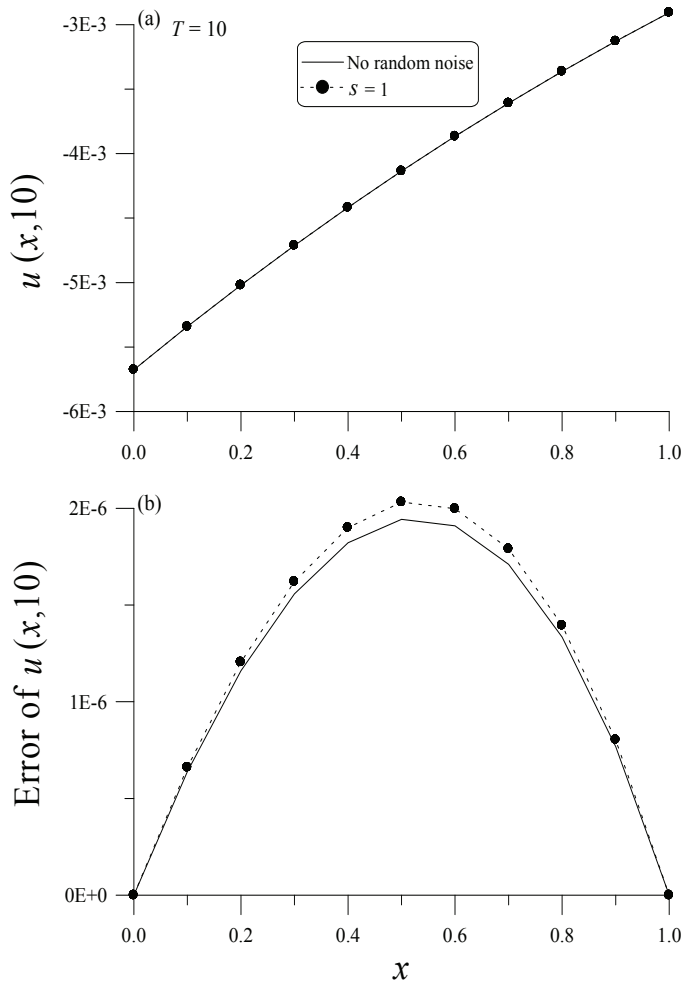


Figure 5: Comparisons of numerical solutions were made in (a) with different levels of noise $s = 0, 1$, and (b) the corresponding numerical errors.

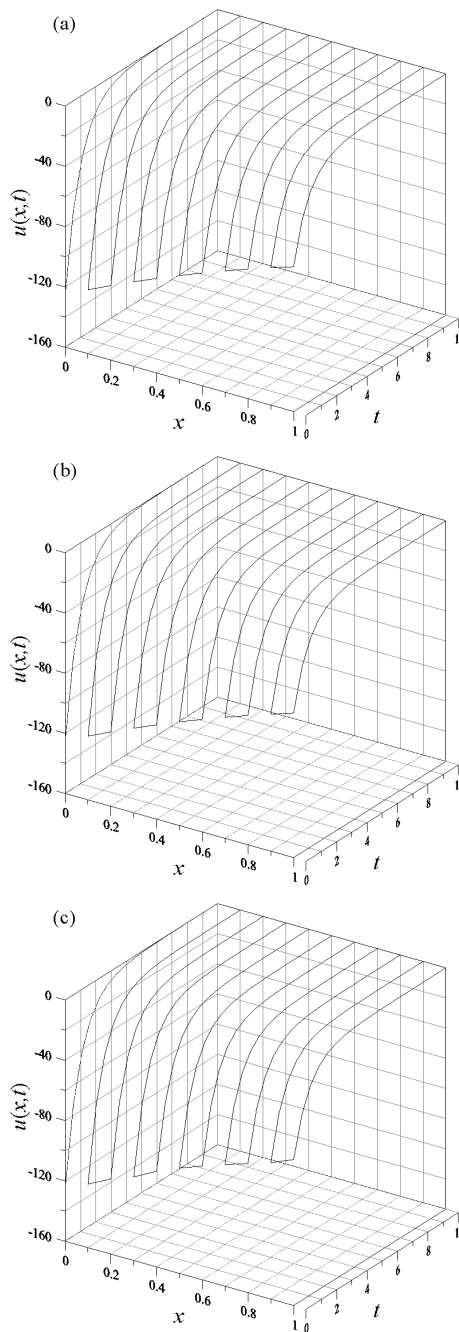


Figure 6: The exact solution for Example 2 of one-dimensional nonlinear HCP with $T = 10$ are shown in (a), in (b) the OVDA solution without random noise effect, and in (c) the OVDA solution with random noise.

with the boundary conditions

$$u(0,t) = 729e^{-2t}, u(1,t) = 64e^{-2t}, \quad (61)$$

and the initial condition

$$u(x,0) = (x-3)^6. \quad (62)$$

The exact solution is

$$u(x,t) = (x-3)^6 e^{-2t}. \quad (63)$$

By employing the present approach to resolve the above equation in the domain of $0 \leq x \leq 1$ and $0 \leq t \leq 3$, we utilize $n_1 = 26$ and $n_2 = 6$, which are numbers of nodal points in a standard finite difference approximation of Eq. (60). Because a_0 defined in Eq. (18) is a very important factor of our new method, we demonstrate it in Fig. 7(b) for the present scheme with $\gamma = 0$, when the residual error is drawn in Fig. 7(a), and α is shown in Fig. 7(c) by the dashed lines. Under a convergence criterion $\varepsilon = 0.1$, the proposed scheme with $\gamma = 0$ can also converge with 996 steps, and acquires an accurate solution with the maximum error 4.79×10^{-3} . The optimal α varies in a narrow band with the range from 0.9999 to 1.0000, and a_0 approaches to a constant, which finds an attracting set for the iterative orbit. Under the same convergence criterion, the present algorithm with $\gamma = 0.17$ converges much fast with only 465 steps. The residual error, a_0 and α are shown in Fig. 7 by the solid lines. By employing $\gamma = 0.17$ the value of a_0 does not tend to a constant, and its value is smaller than the a_0 acquired from the present algorithm with $\gamma = 0$ and optimal α , which is the main reason to cause the fast convergence of the new method with $\gamma = 0.15$.

In this example, when the input initial measured data are disturbed by random noise, we are interested in the stability of OVDA, which is investigated by adding the level of random noise on the final data. The results of $T = 3$ are compared with the numerical result without contemplating the absolute random noise in Fig. 8. Note that the absolute noise level with $s = 1$ perturbs the numerical solutions a little from that without adding the noise, and the maximum error is 2.02×10^{-4} . The exact solutions and numerical solutions are drawn in Figs. 9(a)-(c) sequentially. Even under the large noise, the numerical solution indicated in Fig. 9(c) is a good approximation to the exact initial data as displayed in Fig. 9(a).

5 Conclusions

We proved that the proposed scheme is convergent automatically, and without calculating the inversions of the Jacobian matrices. It can resolve a large system of

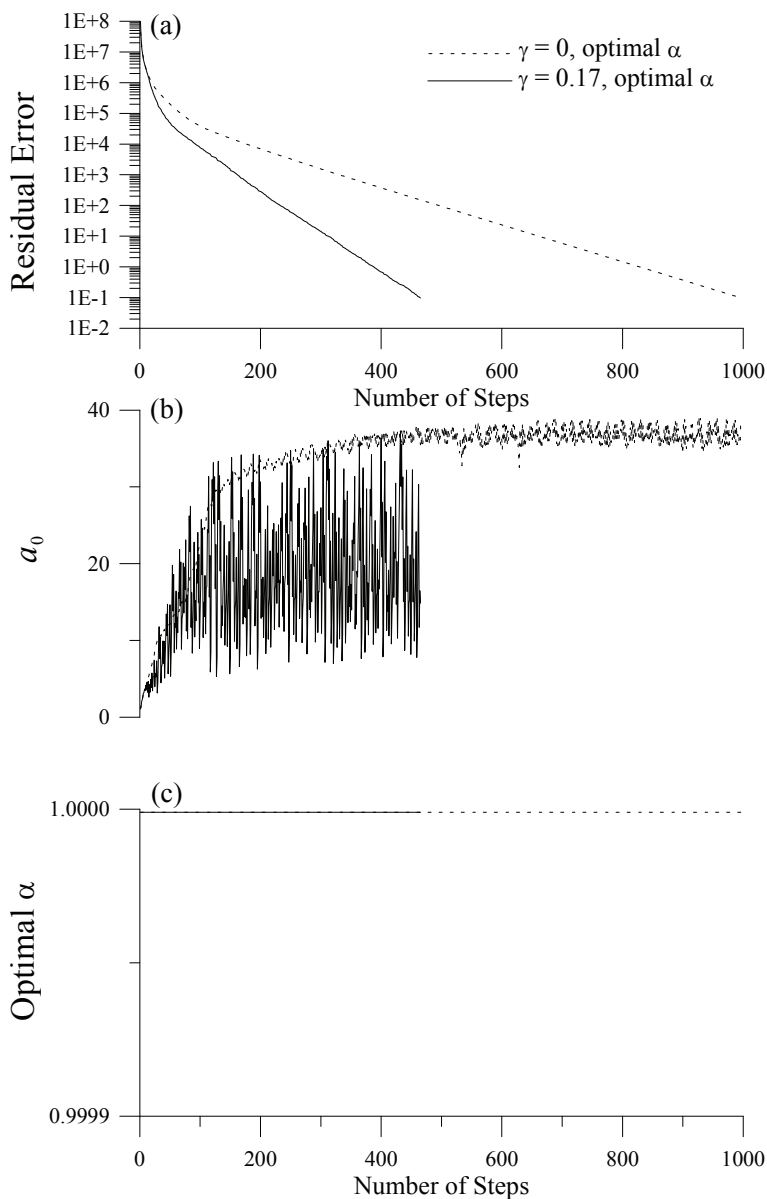


Figure 7: For example 3, with different α and γ , comparing residual errors, α_0 and α .

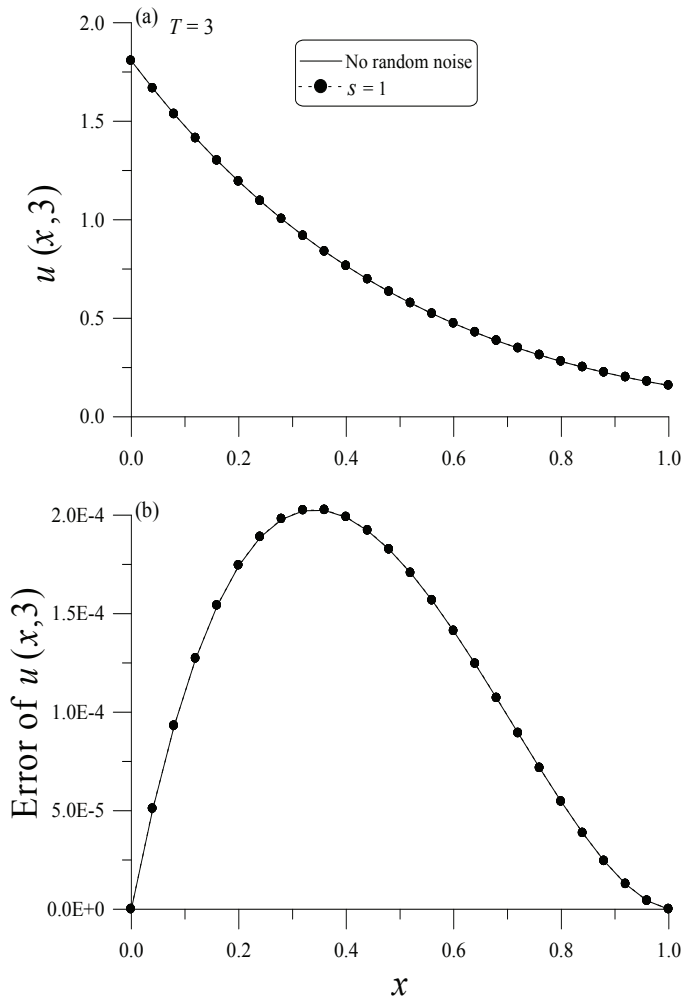


Figure 8: Comparisons of numerical solutions were made in (a) with different levels of noise $s = 0, 1$, and (b) the corresponding numerical errors.

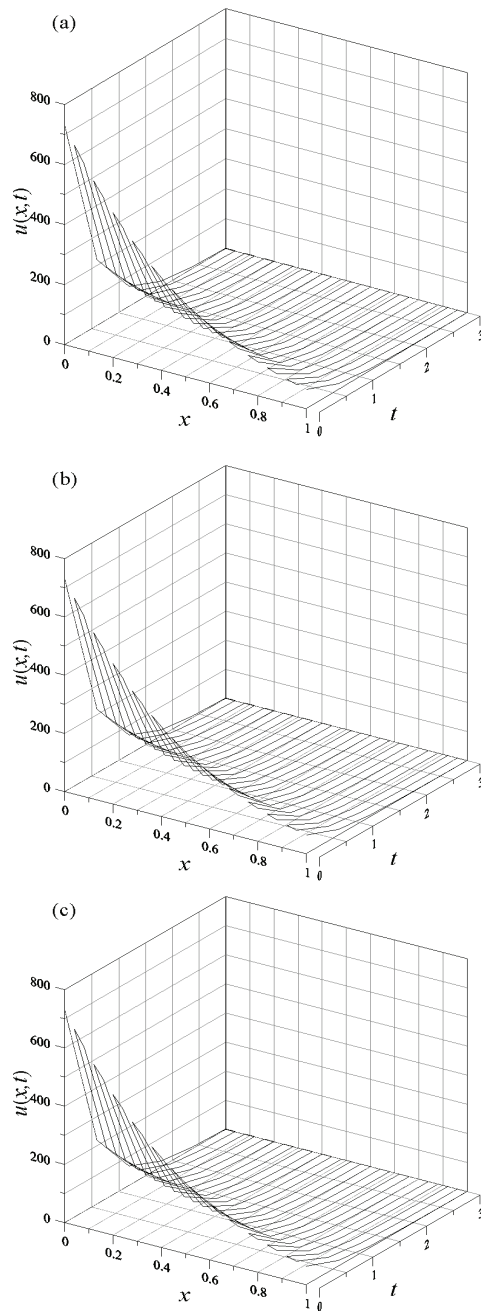


Figure 9: The exact solution for Example 3 of one-dimensional nonlinear HCP with $T = 3$ are shown in (a), in (b) the OVDA solution without random noise effect, and in (c) the OVDA solution with random noise.

nonlinear algebraic equations very quickly. On the basis of those numerical experiments, we exhibit that the OVDA is applicable to the nonlinear HCPs, and validate the accuracy and efficiency of the proposed approach. Two mechanisms for improving the convergence speed of the present method were discovered. For some problems merely the employment of the bifurcation parameter $\gamma > 0$, or merely the utilization of the optimization parameter α is already enough to accelerate the convergence speed. Furthermore, when both the effects of optimization and bifurcation were utilized in all the examined problems, we can obtain high efficient and accurate results.

Acknowledgement: The first and corresponding author would like to express his thanks to the National Science Council, ROC, for their financial supports under Grant Numbers, NSC 100-2221-E492-018.

References

- Bialecki, R. A.; Jurgas, P.; Kuhn, G.** (2002): Dual reciprocity BEM without matrix inversion for transient heat conduction. *Eng. Anal. Bound. Elem.*, vol. 26, pp. 227–236
- Bulgakov, V.; Sarler, B.; Kuhn, G.** (1998): Iterative solution of systems of equations in the dual reciprocity boundary element method for the diffusion equation. *Int. J. Numer. Meth. Eng.*, vol. 43, pp. 713–732.
- Chang, C.-W.; Liu, C.-S.** (2010): A new algorithm for direct and backward problems of heat conduction equation. *Int. J. Heat Mass Transfer*, vol. 53, pp. 5552–5569.
- Chantasiriwan, S.** (2006): Methods of fundamental solutions for time-dependent heat conduction problems. *Int. J. Numer. Meth. Eng.*, vol. 66, pp. 147–165
- Chu, H. P.; Chen, C. L.** (2008): Hybrid differential transform and finite difference method to solve the nonlinear heat conduction problem. *Commun Nonlinear Sci. Numer Simul.*, vol. 13, pp. 1605–1614
- Johansson, B. T.; Lesnic, D.** (2008): A method of fundamental solutions for transient heat conduction. *Eng. Anal. Bound. Elem.*, vol. 32, pp. 697–703
- Liu, C.-S.** (2000): A Jordan algebra and dynamic system with associator as vector field. *Int J Non-Linear Mech*, vol. 35, pp. 421–429.
- Liu, C.-S.; Atluri, S. N.** (2011a): Simple "residual-norm" based algorithms, for the solution of a large system of non-linear algebraic equations, which converge faster than the Newton's method. *CMES: Computer Modeling in Engineering & Sciences* vol. 71, pp. 279–304.

- Liu, C.-S.; Atluri, S. N.** (2011b): An iterative algorithm for solving a system of nonlinear algebraic equations, $\mathbf{F}(\mathbf{x}) = 0$, using the system of ODEs with an optimum α in $\dot{x} = \lambda[\alpha F + (1 - \alpha)B^T F]$; $B_{ij} = \partial F_i / \partial x_j$. *CMES: Computer Modeling in Engineering & Sciences*, vol. 73, pp. 395–431.
- Moore, P. K.** (1994): A posteriori error estimation with finite element semi- and fully discrete methods for nonlinear parabolic equations in one space dimension. *SIAM J. Numer. Anal.*, vol. 31, pp. 149–169
- Necati Özisik, M.** (1994): *Finite Difference Methods in Heat Transfer*, BocaRaton, CRC Press.
- Sutradhar, A.; Paulino, G. H.; Gray, L. J.** (2002): Transient heat conduction in homogeneous and non-homogeneous materials by the Laplace transform Galerkin boundary element method. *Eng. Anal. Bound. Elem.*, vol. 26, pp. 119–132.
- Walker, S. P.** (1992): Diffusion problems using transient discrete source superposition. *Int. J. Numer. Meth. Eng.*, vol. 35, pp. 165–178
- Zerroukat, M.** (1999): A boundary element scheme for diffusion problems using compactly supported radial basis functions. *Eng. Anal. Bound. Elem.*, vol. 23, pp. 201–209.
- Zhu, S. P.** (1998): Solving transient diffusion problems: time-dependent fundamental solution approaches versus LTDRM approaches. *Eng. Anal. Bound. Elem.*, vol. 21, pp. 87–90.
- Zhu, S. P.; Liu, H. W.; Lu, X. P.** (1998): A combination of LTDRM and ATPS in solving diffusion problems. *Eng. Anal. Bound. Elem.*, vol. 21, pp. 285–289.
- Zienkiewicz, O. C.; Taylor, R. L.; Zhu, J. Z.** (2005): *The Finite Element Method: Its Basis and Fundamentals*, Amsterdam, London, Butterworth-Heinemann
- Zokayi, A.R.; Hadizadeh, M.; Darania, P.; Rajabi, A.** (2006): The relation between the Emden–Fowler equation and the nonlinear heat conduction problem with variable transfer coefficient. *Commun Nonlinear Sci. Numer Simul*, vol. 11, pp. 845–853

